전자물리특강: Interfaces & Carrier Injection

Changhee Lee
School of Electrical Engineering and Computer Science
Seoul National Univ.
chlee7@snu.ac.kr

Organic LEDs - Structure

Organic Semiconductor LEDs
(polymers or small molecules)

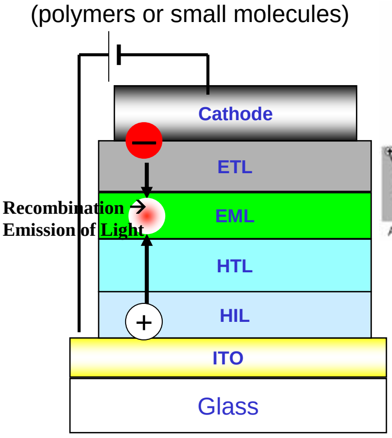

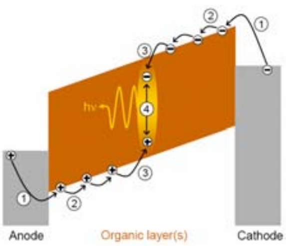

Fundamental processes
(1) Charge injection
(2) Charge carrier transport
(3) Exciton formation
(4) Recombination

Inorganic Semiconductor LEDs
(p-n junction LED)

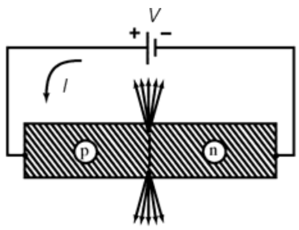

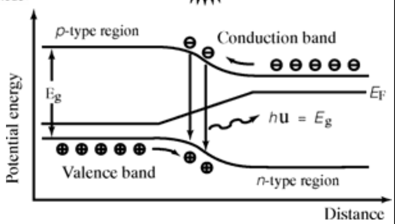

(1) Lower the barrier at electrodes → Efficient and balanced carrier injection
(2) Band offsets between the layers: Space charges build up at heterojunction.
→ High carrier densities & effective *e-h* capture

Electron-hole balance for high efficiency OLED

- Electron-Hole Balance → improved efficiency & Lifetime

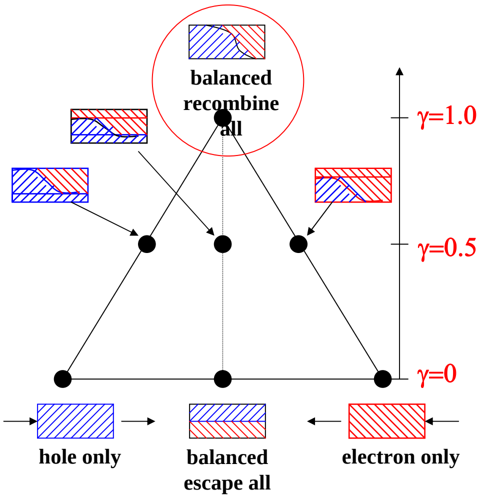

$\eta_\phi = \chi\gamma\beta\phi_L$

χ: coupling-out factor

γ: charge balance factor

β: probability of production of emissive species

ϕ_L: quantum efficiency of luminescence

High efficiency OLED requires:
- Efficient injection of holes/electrons at electrodes
- Balance of electrons and holes in the EML
- Efficient radiative recombination of e-h pairs
- Confinements of produced excitons

- Ambipolar emitting layer
- Mixed emitting layer (co-doped host)
- p-type or n-type doping at the electrode interface

J. C. Scott et al., SPIE 3476, 111 (1998)

Metal/Organic Interfaces

전자물리특강
2007. 2학기

Schottky-Mott Model

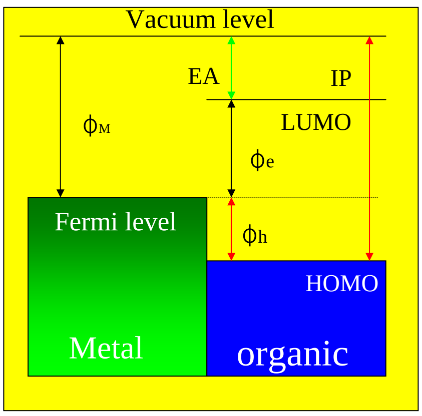

- No interface interaction &Vacuum level alignment
- Injection barriers estimated with the bulk parameters of individual materials

ϕ_h=IP-ϕ_M, ϕ_e=ϕ_M-EA

Interface Dipole Model

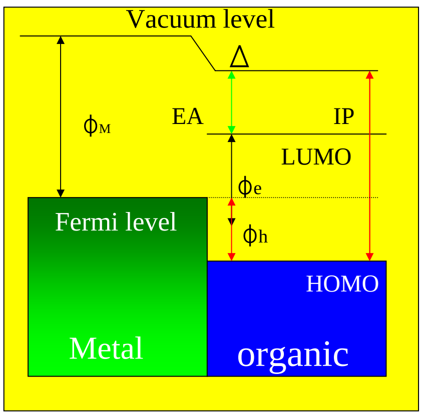

- Common vacuum level assumption is not valid
- A dipole (Δ) exists at metal/organic interface

Φ_h=IP-Φ_M+Δ
Φ_e=Φ_M-EA-Δ

Prof. S. T. Lee, ICEL-5

Organic Semiconductor Lab
Changhee Lee, SNU, Korea

Fermi level alignment at the metal/semiconductor contact

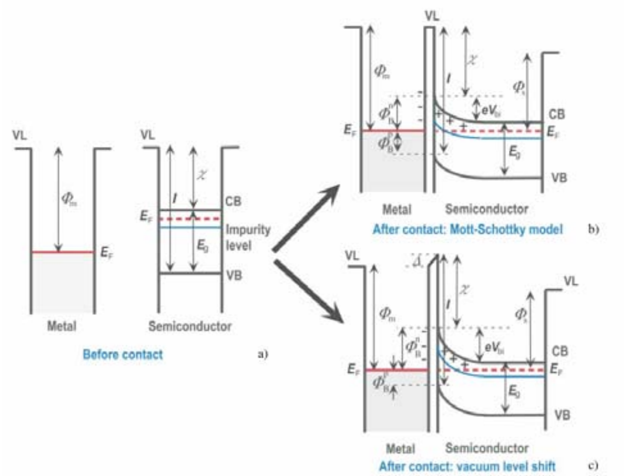

ϕ_m: 금속의 work function
ϕ_s : 반도체의 work function
χ:electron affinity

Barrier height for e injection
$\Phi_{Bn} = \Phi_m - \chi$

built-in potential
$eV_{bi} = |\Phi_m - \Phi_s|$

Formation of interface dipole inducing vacuum level shift (Δ)
→ Barrier height is modified: $\Phi_{Bn} = \Phi_m + \Delta - \chi$
→ V_{bi} is also modified: $eV_{bi} = |\Phi_m + \Delta - \Phi_s|$

Workfunction & IP Measurement: Photoelectric effect

전자물리특강
2007. 2학기

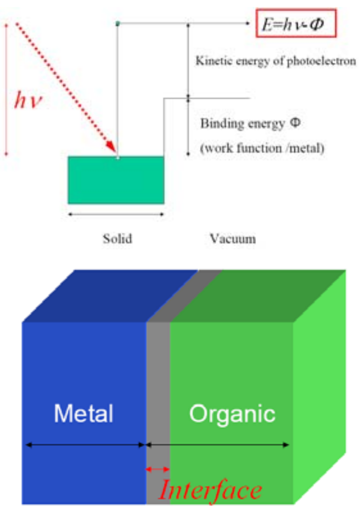

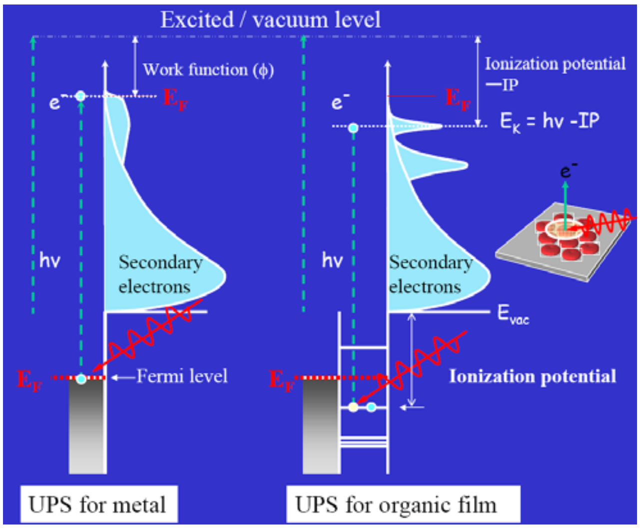

Energy level alignment at interface: Molecular orientation, reaction with metal, distortion of electronic distribution, existence of electric dipoles, etc.

Organic Semiconductor Lab
Changhee Lee, SNU, Korea

STM-excited EL and spectroscopy on organic materials

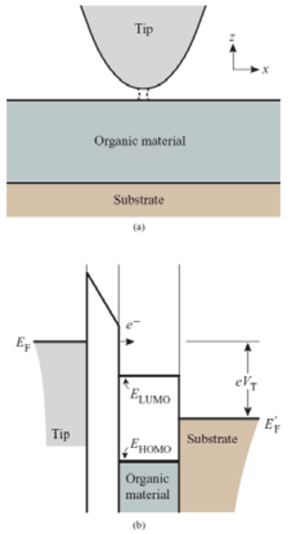

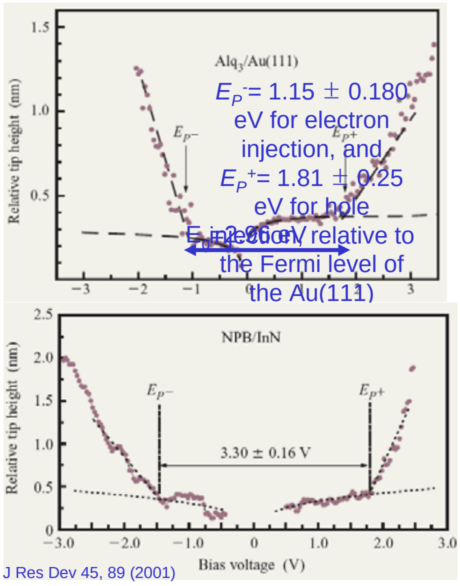

E_P^-= 1.15 ± 0.180 eV for electron injection, and E_P^+= 1.81 ± 0.25 eV for hole injection relative to the Fermi level of the Au(111)

E_g = 2.96 eV

S. F. Alvarado, L. Rossi, P. Muller, P. F. Seidler, W. Riess, IBM J Res Dev 45, 89 (2001)

Origin of interface dipole

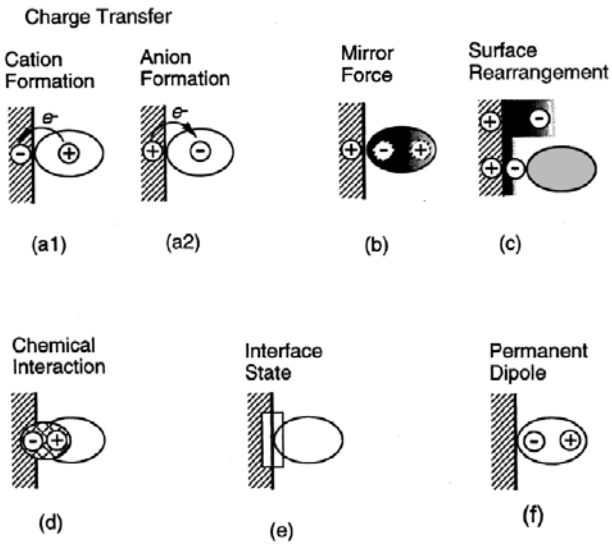

Possible factors forming and affecting the interfacial dipole layer.
a1) and a2): Charge transfer across the interface,
b) Concentration of electrons in the adsorbate leading to positive charging of the vacuum side,
c) Rearrangement of electron cloud at the metal surface, with the reduction of tailing into vacuum,
d) Strong chemical interaction between the surface and the adsorbate leading to the rearrangement of the electronic cloud and also the molecular and surface geometries (both directions of dipoles possible),
e) Existence of interface state serving as a buffer of charge carriers,
f) Orientation of polar molecules or functional groups.

H. Ishii, K. Sugiyama, E. Ito, and K. Seki, Adv. Mater. **11**, 605 (1999).

Potential barrier at metal/Alq3 interfaces

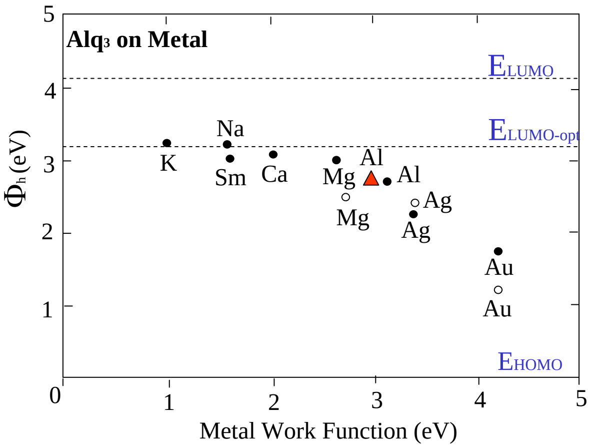

Tang, Lee, et al. Chem. Phys. Lett, 396, 92 (2004)
Hill et al. Appl. Phys. Lett. 73, 662 (1998)
Isjii et al. Adv. Mater. 11, 605 (1999)

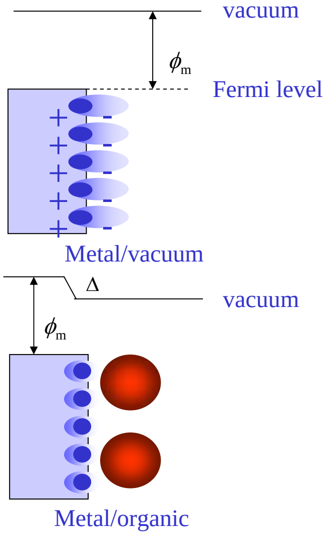

Part of the tailing of electrons at the material surface is compressed back into the metal.
→ Interface dipole Δ is formed.

(PEDOT or Metal)/Organic Interface

전자물리특강
2007. 2학기

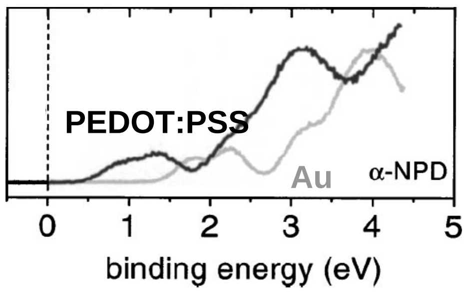

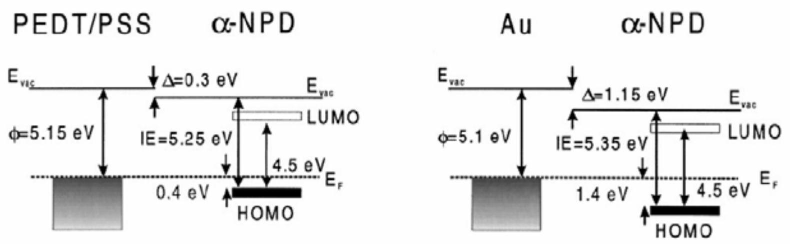

N. Koch, A. Kahn, J. Ghijsen and J.-J. Pireaux, J. Schwartz, R. L. Johnson, A. Elschner, Appl. Phys. Lett. **82**, 70 (2003)

Organic Semiconductor Lab
Changhee Lee, SNU, Korea

Energy levels of Organic Materials

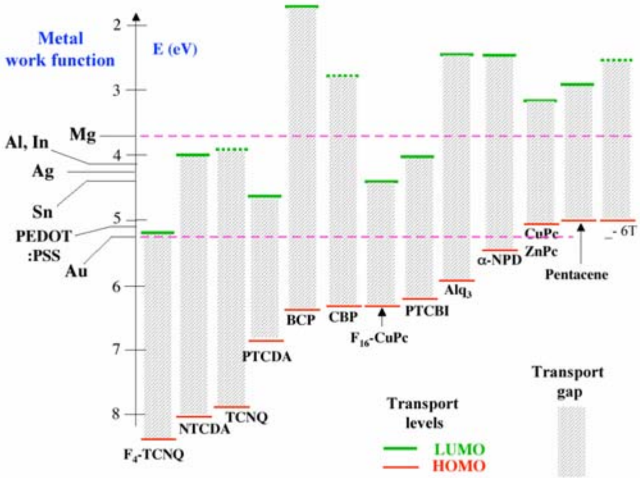

Weiying Gao and Antoine Kahn (Princeton Univ.), NSF workshop, "Technological Challenges for Flexible, Light-weight, Low-cost and Scalable Organic Electronics and Photonics," January 16-17, 2003

Ionization Potential (eV)

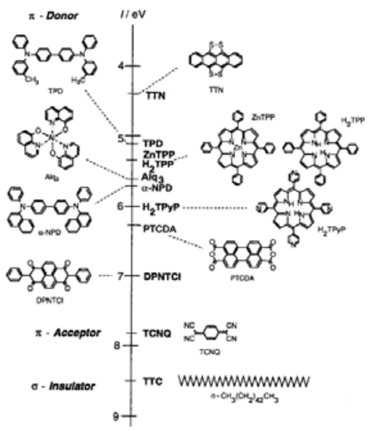

H. Ishii, K. Sugiyama, E. Ito, and K. Seki, Adv. Mater. **11**, 605 (1999).

Electroabsorption

Electroabsorption Measurement

a.c. Field $E = E_{dc} + E_{ac}\cos(\Omega t)$

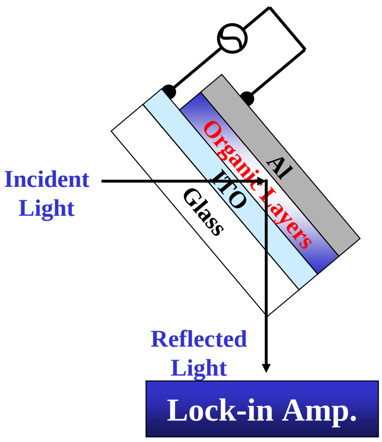

Electroabsorption response to an E field

$$\Delta\alpha(h\nu) \propto -\frac{\Delta T}{T}(h\nu) \propto \mathrm{Im}\,\chi^{(3)}(h\nu)E^2$$

The areal charge density at each interface:

$$\sigma = \frac{1}{4\pi}\Delta(\varepsilon E_{dc})$$

σ = areal charge density
ε = dielectric constant,
Edc = electric field
Δ = difference between the two layers

Electroabsorption

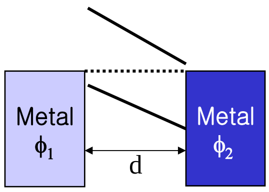

No DC Bias
Internal Field = $(\phi_1-\phi_2)/d$

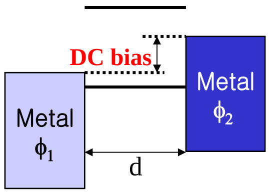

DC bias = $(\phi_1-\phi_2)/d$
Internal Field = 0

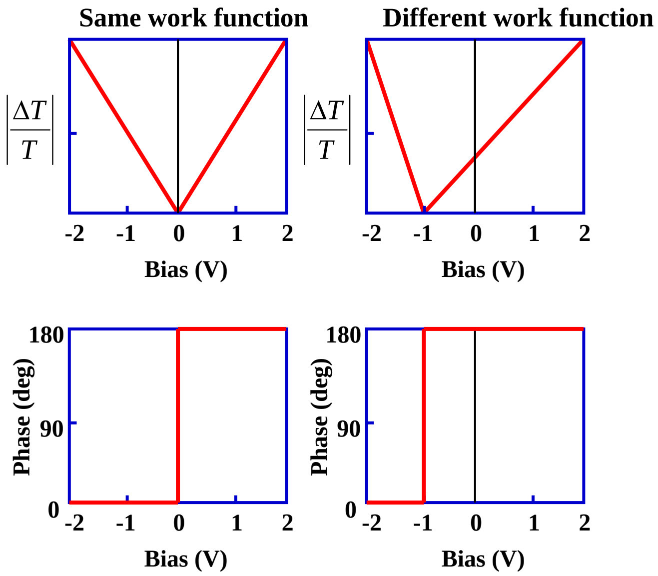

Measurement of an internal electric field

Al/MEH-PPV/Al

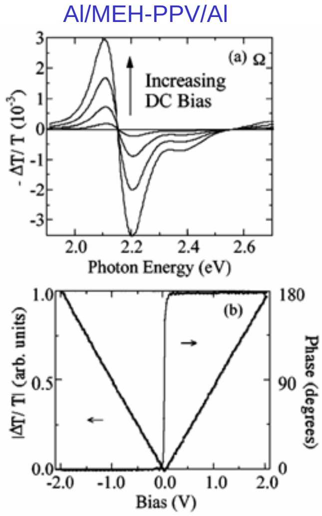

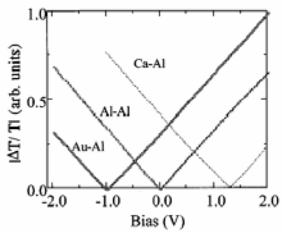

FIGURE 5. Magnitude of the electroabsorption response at 2.1 eV as a function of bias for three metal/MEH-PPV/Al structures.

TABLE 1. Work Function Difference, $\Delta\phi$, and Electro-absorption Zero Field Bias, V_0, for a Series of Metal Contact Pairs to MEH-PPV

Contact metals	$\Delta\phi$	V_0
Au–Al	−0.8	−1.0
Al–Al	0.0	0.0
Ca–Al	1.4	1.3
Sm–Al	1.6	1.3
Ag–Ca	1.4	1.4
Cu–Ca	1.7	1.7
Au–Ca	2.2	2.0
Pt–Ca	2.7	2.1

Ian H. Campbell, John P. Ferraris, Thomas W. Hagler, Michael D. Joswick, Ian D. Parker, Darryl L. Smith
Polymers for Advanced Technologies, **8** (7), pp. 417 – 423

Internal electric field and accumulated charges

MULTILAYER ORGANIC LED

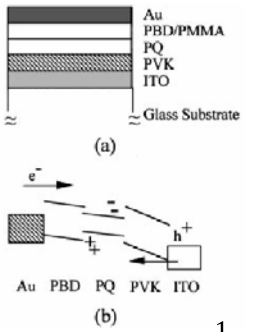

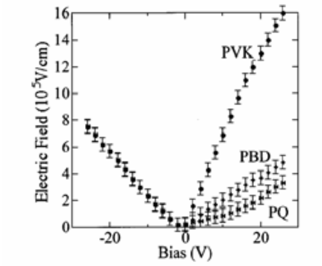

FIGURE 9. Electric field as a function of d.c. bias voltage in each layer of the LED. The a.c. bias amplitude was 3 V.

$$\sigma = \frac{1}{4\pi}\Delta(\varepsilon E_{dc})$$

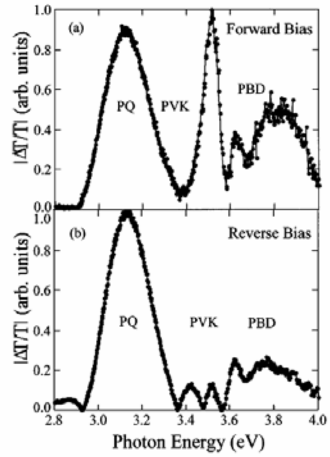

FIGURE 8. Electroabsorption spectra of the three layer LED under (a) 20 V forward bias and (b) −20 V reverse bias at the fundamental frequency of the applied a.c. bias. The relative changes in the amplitudes of the signal from each layer are evident. The a.c. bias amplitude was 3 V.

At the largest forward bias voltage measured,
electron density at the PQ/PVK interface: 2×10^{12} electrons/cm^2

hole density at the PBD/PQ interface: 3×10^{11} holes/cm^2.

Photovoltaic measurement of the built-in potential

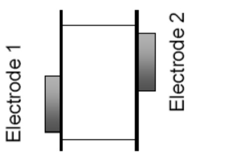

Open circuit conditions

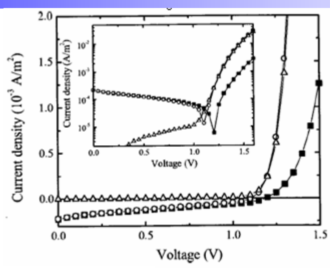

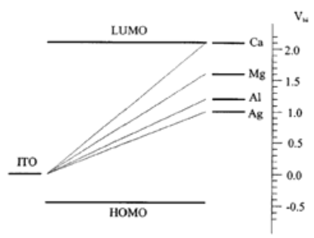

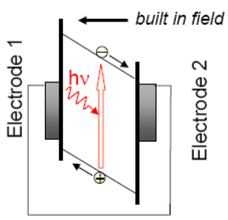

Short circuit conditions

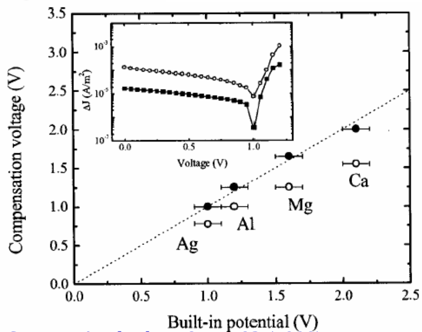

G. G. Malliaras, J. R. Salem, P. J. Brock, and J. C. Scott, J. Appl. Phys. **84**, 1583 (1998)

Effect of Cu-PC buffer layer on the efficiency and driving voltage

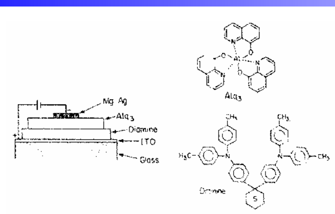

FIG. 1. Configuration of EL cell and molecular structures.

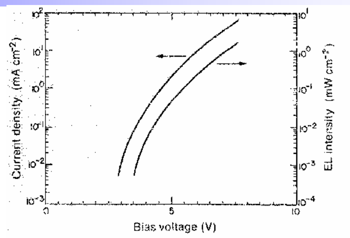

FIG. 2. Brightness-current-voltage characteristics of an ITO/diamine/Alq_3/Mg:Ag EL cell.

1.5 lm/W

C. W. Tang and S. A. Van Slyke, Appl. Phys. Lett. **51**, 913 (1987)

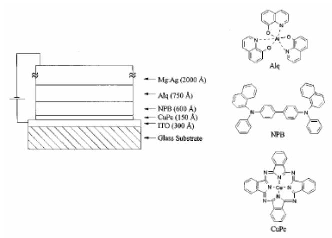

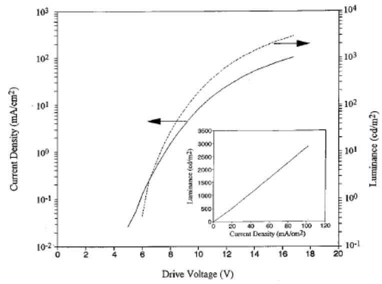

2.8 cd/A

0.73 lm/W

S. A. Van Slyke, C. H. Chen, and C. W. Tang, Appl. Phys. Lett. **69**, 2160 (1996)

Effect of Cu-PC buffer layer on the hole injection and EL efficiency

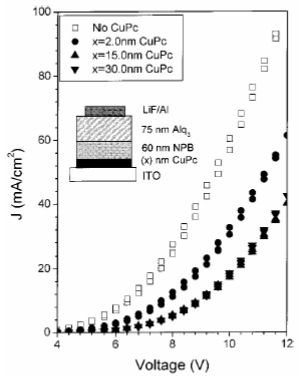

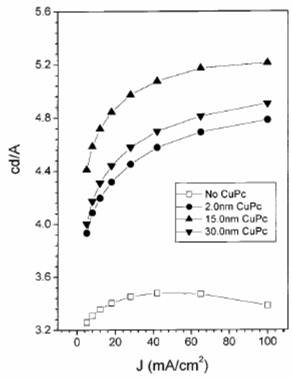

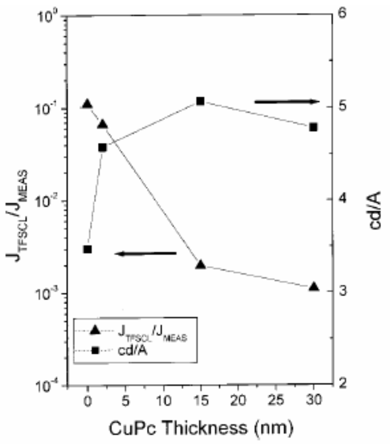

$$\text{Injection efficiency}: \ \eta = \frac{\text{injected current}}{SCLC}$$

$\eta = 1$ for ohmic contact

$\eta < 1$ for current-limiting contact

$$J_{SCLC} = \frac{9}{8}\frac{\varepsilon_o \varepsilon_r \mu V^2}{d^3}$$

Cu-PC reduces hole injection efficiency

→ Improved balance between *e* and *h* currents

→ Increase the efficiency

E. W. Forsythe, M. A. Abkowitz, and Yongli Gao, *J. Phys. Chem. B*, **104**, 3948 (2000)

Hole Injection Materials - PEDOT:PSS

Chemical name: Poly(3,4-ethylenedioxythiophene) poly(styrenesulfonate) aqueous dispersion

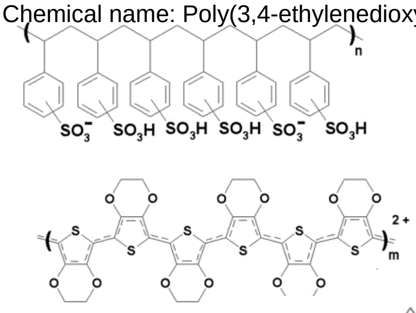

Baytron® P VP AI 4083

H.C. Starck

Physical Data of Baytron P VP AI 4083

Solid Content ~1,5 %

Viscosity ~ 12 mPas

Particle Size (swollen) d 50 < 80 nm

Particle Size (swollen) d 90 < 100 nm

Resistivity (dried layer) 1000 W cm

Properties and Applications of Baytron P VP AI 4083

Baytron P VP AI 4083 has been developed particularly for use as a hole-injection layer in OLEDs. Baytron P VP AI 4083 has smaller particles than the standard version of Baytron P. Accordingly, smoother layer surfaces can be obtained, and electric "shorts" in the polymer LED devices can be reduced.

Notes on using Baytron P VP AI 4083

Baytron P VP AI 4083 is preferably applied by spin-coating. Filtration of the dispersion through a 0.45 µm membrane filter is recommended before use. The coatings are dried at a maximum temperature of 200°C for 1 minute, but a temperature between 100°C and 150°C is usually sufficient. The optimal thickness of the dried layer is in the range of 50 to 250 nm.

Compared to devices without an interfacial Baytron P layer:
- The operation voltage can be reduced.
- The light efficiency is increased.
- The lifetime of the display is increased.

http://www.hcstarck.de/

Hole Injection Materials - PEDOT:PSS

Workfunction of PEDOT/PSS

Results UPS:

AI4071 (PEDT:PSS 1:2.5)
AI4083 (PEDT:PSS 1:6)
CH8000 (PEDT:PSS 1:20)

Φ = 5.1 - 5.2 eV

OLED-Setup:

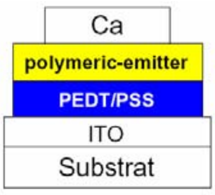

@ 4V	L [cd/m²]	η [cd/A]
with PEDT/PSS	10800	5.9
without	1000	2.9

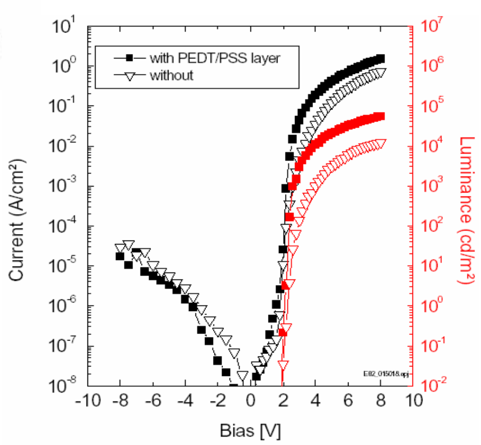

Andreas Elschner, H.C.Starck, Micro Symposium 2002 Cologne, December 9th

Electron injection layer

Enhanced electron injection in organic electroluminescence devices using an Al/LiF electrode

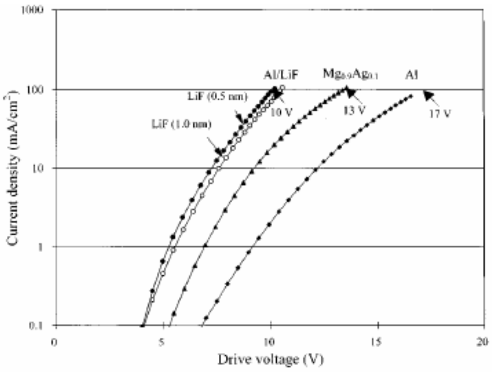

FIG. 1. Current–voltage characteristics of three EL devices using an Al, a $Mg_{0.9}Ag_{0.1}$, and an Al/LiF electrode, respectively.

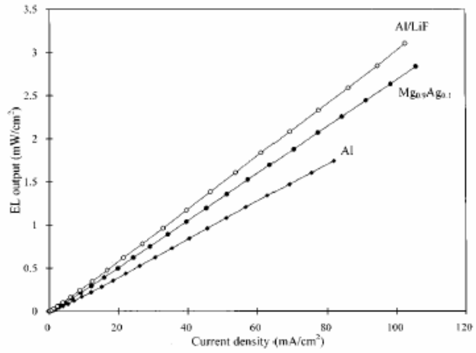

FIG. 3. Light-current characteristics of three EL devices using Al, $Mg_{0.9}Ag_{0.1}$, and Al/LiF electrodes, respectively.

L. S. Hung, C. W. Tang, and M. G. Mason, APL **70**, 152, (1997)

Cathode Materials

전자물리특강
2007. 2학기

1987 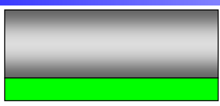 **Mg:Ag**

C. W. Tang and S. A. VanSlyke, Appl. Phys. Lett. **51**, 913 (1987)

1990 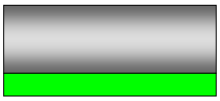 **Al:Li**

Y. Itoh, N. Tomikawa, S. Kobayashi, and T. Minato, Extended Abstracts,The 51th Autumn Meeting, The Japan Society of Applied Physics (1990), p. 1040.
T. Wakimoto, et al, EL '94 (1994), p. 77.
T. Wakimoto, Y. Fukuda, K. Nagayama, A. Yokoi, H. Nakada, and M. Tsuchida, IEEE Trans. Electron Devices 44, 1245 (1997).

1993 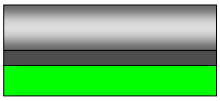 **Ag**
Li

J. Kido, K. Nagai, and Y. Okamoto, IEEE Trans. Electron Devices **40**, 1342 (1993).

1997  **Al**
Li
Al

E. I. Haskal, A. Curioni, P. F. Seidler, and W. Andreoni, Appl. Phys. Lett. **71**, 1151 (1997)

1997 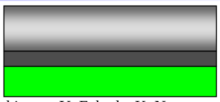 **Al**
Li2O, LiF , MgF2, NaCl

T. Wakimoto, Y. Fukuda, K. Nagayama, A. Yokoi, H. Nakada, and M. Tsuchida, IEEE Trans. Electron Devices **44**, 1245 (1997).
L. S. Hung, C. W. Tang, and M. G. Mason, Appl. Phys. Lett. **70**, 152 (1997).
C. H. Lee, Synth. Met (1997) MgF2

1998 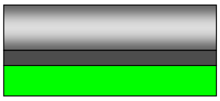 **Al**
Al:LiF, Al:CsF composite

G. E. Jabbour, B. Kippelen, N. R. Armstrong, and N. Peyghambarian, Appl. Phys. Lett **73**, 1185 (1998)

1998 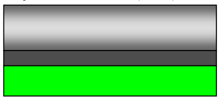 **Al**
Liq, Lidpm

J.Kido et al., El Workshop. Oregon (1998)

1998 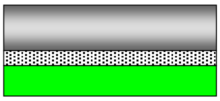 **Al**
Li-doped Organics

Junji Kido, Toshio Matsumoto, Appl.Phys. Lett. **73**, 2866 (1998)

Dynamic p/n junction

Light-emitting electrochemical cell (LEC)

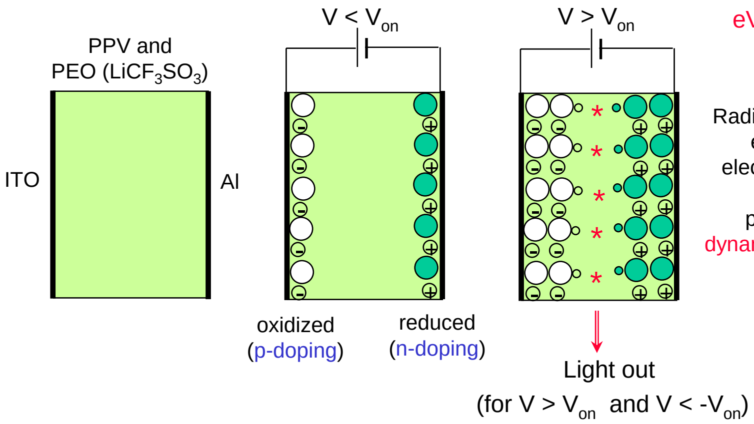

$eV_{on} = E_g$

Radiative decay of e-h pairs in electrochemically induced p-n junction: dynamic & reversible

Q. Pei, Y. Yang, C. Zhang, and A. J. Heeger, *J. Am. Chem. Soc.* **118**, 3922 (1996)

Control of injection via electrical doping

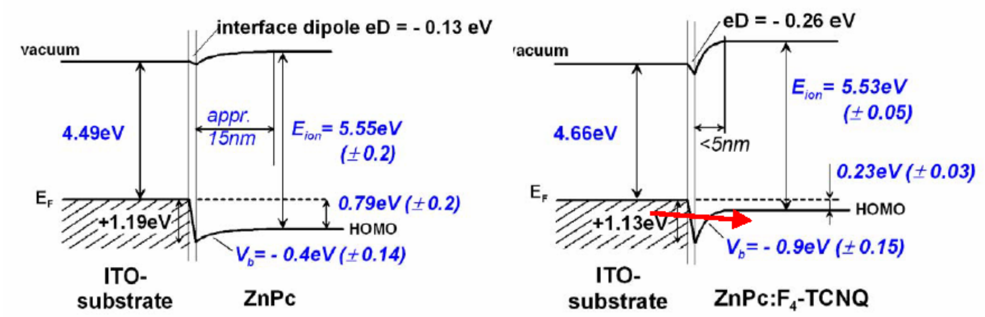

Undoped: blocking

Doped: Ohmic

matrix

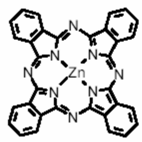

ZnPc

dopant

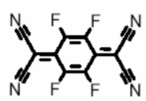

F_4-TCNQ

J. Blochwitz et al., Organic Electronics **2**, 97 (2001)

Electronic structure of ZnPc and F4-TCNQ

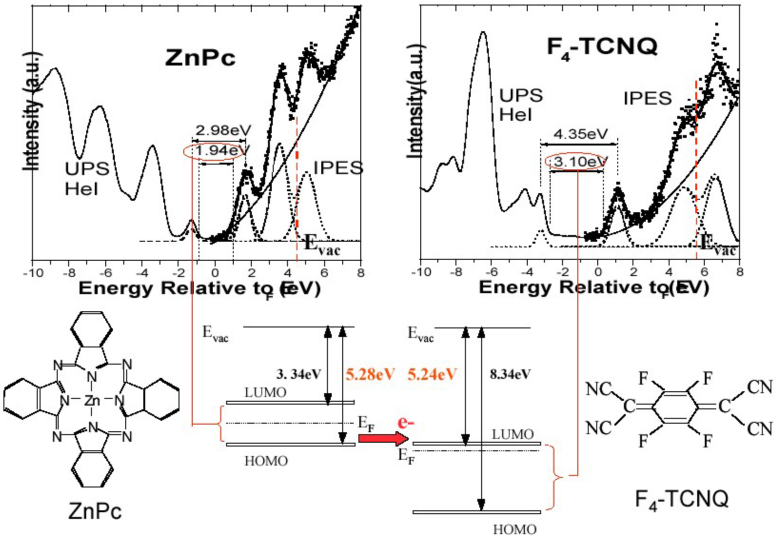

W. Gao and A. Kahn, Appl.Phys.Lett., **79**, 4040 (2001)

electrical doping

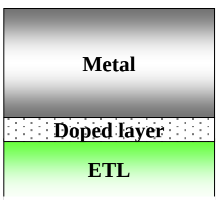

- Realize ohmic contact
- Increase conductivity

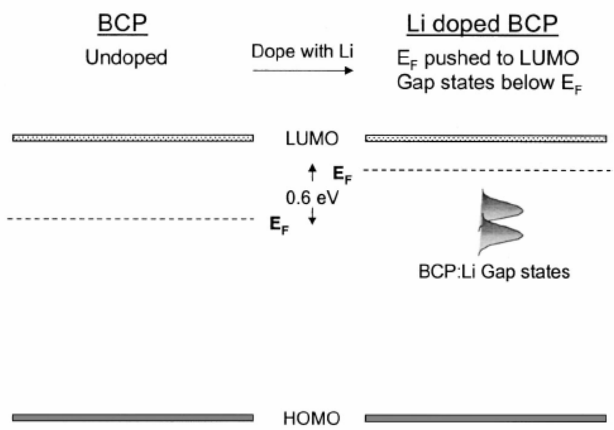

Recent work on doping of molecular films

p-type doping

- PC-TPD-DEG: TBAHA, A. Yamamori et al. Appl. Phys. Lett. **72**, 2147 (1998)
- VOPc: F4-TCNQ, J. Blochwitz, M. Pfeiffer, T. Fritz, and K. Leo, Appl. Phys. Lett. **73**, 729 (1998)
- TPD: SbCl5, C. Ganzorig and M. Fujihira, Appl. Phys. Lett. **77**, 4211 (2000)
- ZnPc: F4-TCNQ, J. Blochwitz, T. Fritz, M. Pfeiffer, K. Leo, D.M. Alloway, P.A. Lee, N.R. Armstrong, Organic Electronics, **2**, 97-104, (2001)
- ZnPc: F4-TCNQ, W. Gao and A. Kahn, Appl. Phys. Lett. **79**, 4040 (2001); W. Gao and A. Kahn, Organic Electronics 3, 53 (2002); Gao et al. J. Appl. Phys. (2002)
- TDATA:F4-TCNQ, X. Zhou, M. Pfeiffer, J. Blochwitz, A. Werner, A. Nollau, T. Fritz, and K. Leo, Appl. Phys. Lett. 78, 410 (2001)
- MTDATA:F4-TCNQ J. Huang, M. Pfeiffer, A. Werner, J. Blochwitz, S. Liu, and K. Leo, Appl. Phys. Lett. 80, 139 (2002)
- _-NPD: F4-TCNQ, Gao et al., J. Appl. Phys. (2003)

n-type doping

- Li doped Alq3 , Junji Kido, Toshio Matsumoto, Appl.Phys. Lett. **73**, 2866 (1998)
- Alkalimetal benzoate, e.g., C6H5COOLi, between (Alq3) Al, C. Ganzorig and M. Fujihira, Jpn. J. Appl. Phys., Part 2 38, L1348 (1999)
- NTCDA: BEDT-TTF, A. Nollau, M. Pfeiffer, T. Fritz, K. Leo, J. Appl. Phys. 87, 4340 (2000)
- Li doped BCP, G. Parthasarathy, C. Shen, A. Kahn, and S. R. Forrest, J. Appl. Phys. 89, 4986 (2001)
- Li doped BCP (p-i-n); J. Huang, M. Pfeiffer, A. Werner, J. Blochwitz, S. Liu, and K. Leo, Appl. Phys. Lett. 80, 139 (2002)
- Pyronin B doped NTCDA, A. G. Werner, F. Li, K. Harada, M. Pfeiffer, T. Fritz, and K. Leo, Appl. Phys. Lett. 82, 4495 (2003)

Metal-Semiconductor Junction

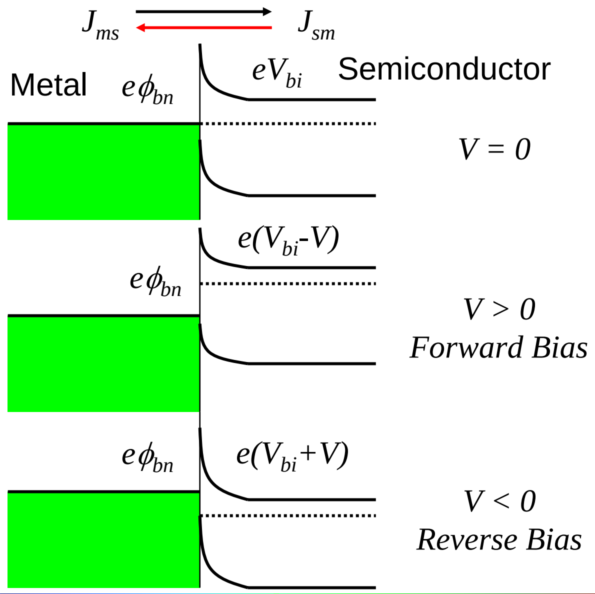

J-V Dependence

$$J = J_s[\exp(\frac{eV}{k_B T}) - 1]$$

$$J_s = A^* T^2 \exp(\frac{-e\phi_{bn}}{k_B T})$$

$$A^* = \frac{4\pi e m_n^* k_B}{h^3}$$

effective Richardson constant for thermionic emission

Carrier Injection

Thermionic Emission

$$J = J_s[\exp(\frac{eV}{k_B T}) - 1]$$

$$J_s = A^* T^2 \exp(\frac{-e\phi_{bn}}{k_B T})$$

effective Richardson constant for thermionic emission

$$A^* = \frac{4\pi e m_n^* k_B}{h^3} = 120(\frac{m^*}{m})\ \mathrm{A/cm^2/K^2}$$

Fowler-Nordheim Tunneling

$$J \approx E^2 \exp(\frac{-b}{E})$$

$$b = \frac{8\pi\sqrt{2m^*}(q\phi)^{3/2}}{3qh}$$

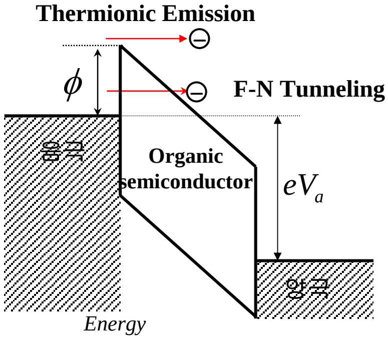

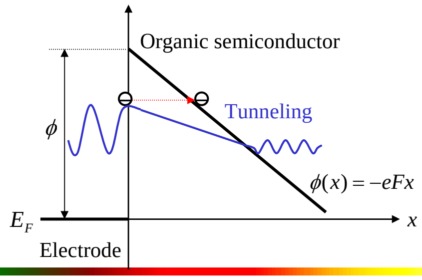

Trap-limited SCLC

Trap-limited SCLC

$$J \propto \mu N_v N_t^{-m} \frac{V^{m+1}}{d^{2m+1}},\quad m = \frac{T_t}{T}.$$

$E_t \approx 0.15\ \mathrm{eV}$

$N_t \approx 10^{18}\ \mathrm{cm^{-3}}$

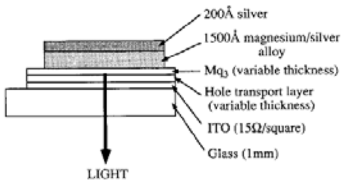

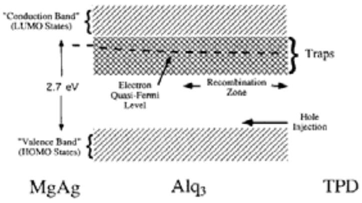

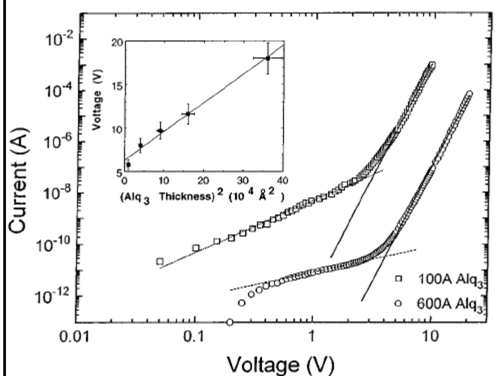

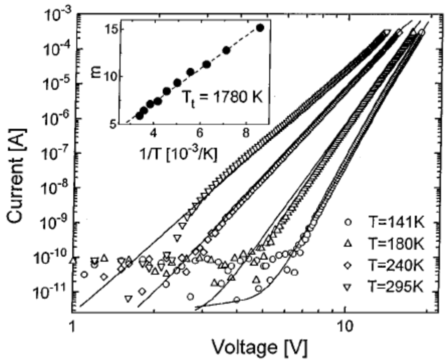

P. E. Burrows, Z. Shen, V. Bulovic, D. M. McCarty, S. R. Forrest, J. A. Cronin and M. E. Thompson, J. Appl. Phys. **79**, 7991 (1996).

Interface-limited injection model

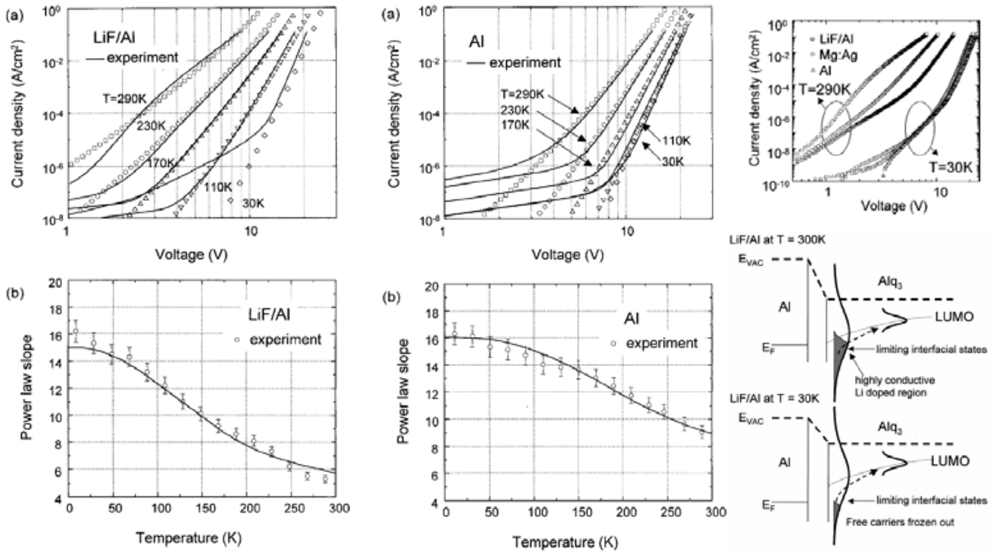

M. A. Baldo and S. R. Forrest, Phys. Rev. B **64**, 085201 (2001)

전자물리특강
2007. 2학기

Interface-limited injection model

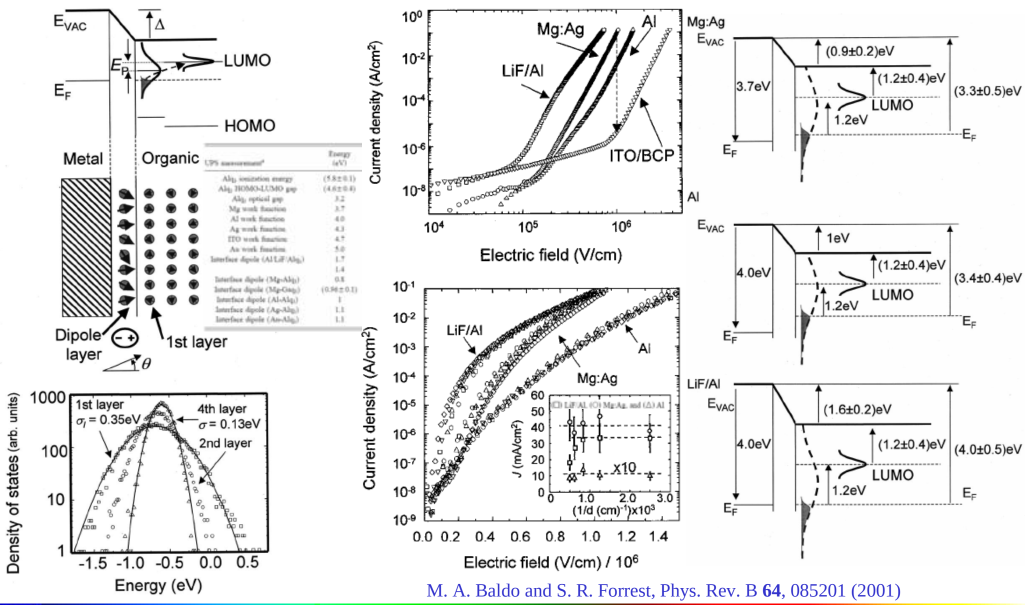

M. A. Baldo and S. R. Forrest, Phys. Rev. B **64**, 085201 (2001)

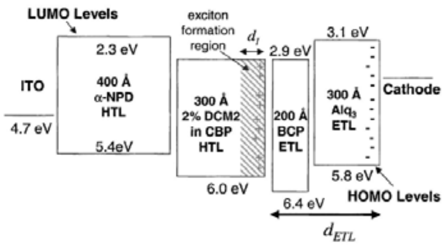

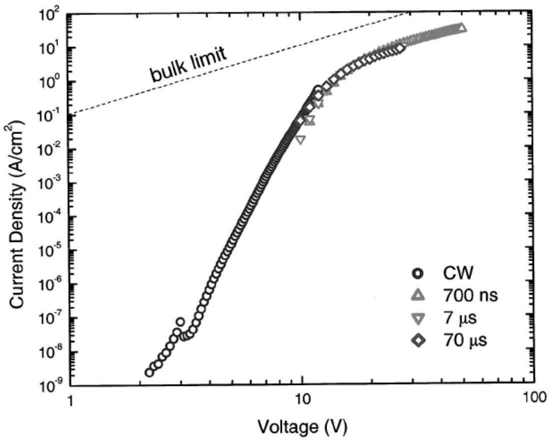

M. A. Baldo, R. J. Holmes, and S. R. Forrest, Phys. Rev. B **66**, 035321 (2002)